*Biochemistry (Moscow), Vol. 70, No. 11, 2005, pp. 1262-1267. Translated from Biokhimiya, Vol. 70, No. 11, 2005, pp. 1534-1540.*
*Original Russian Text Copyright © 2005 by Ugarova, Maloshenok, Uporov, Koksharov.*

# Bioluminescence Spectra of Native and Mutant Firefly Luciferases as a Function of pH

**N. N. Ugarova*, L. G. Maloshenok, I. V. Uporov, and M. I. Koksharov**

*Department of Chemical Enzymology, Faculty of Chemistry, Lomonosov Moscow State University, 119899 Moscow, Russia; fax: (7-095) 939-2660; E-mail: unn@enz.chem.msu.ru*

Received December 2, 2004
Revision received December 27, 2004

**Abstract**—Bioluminescence spectra of the wild-type recombinant *Luciola mingrelica* firefly luciferase and its mutant form with the His433Tyr point mutation were obtained within the pH 5.6-10.2 interval. The spectra are shown to be a superposition of the spectra of the three forms of the electronically excited reaction product oxyluciferin: ketone ($\lambda_{max}$ = 618 nm), enol ($\lambda_{max}$ = 587 nm), and enolate-ion ($\lambda_{max}$ = 556 nm). The shift in $\lambda_{max}$ by 40 nm to the red region in the mutant luciferase bioluminescence at the pH optimum of enzyme activity (pH 7.8) is explained by the change in the relative content of different oxyluciferin forms due to the shift in the ketone ↔ enol ↔ enolate equilibria. A computer model of the luciferase–oxyluciferin–AMP complex was constructed and the structure of amino acid residues participating in the equilibrium is proposed. Computer models of the protein region near the His433 residue for the wild type and mutant luciferases are also proposed. Comparison of the models shows that the His433Tyr mutation increases flexibility of the polypeptide loop that binds the N and C domains of luciferase. As a result, the flexibility of the C domain amino acid residues in the emitter microenvironment increases, and this increase may be the reason for the observed differences in the bioluminescence spectra of the native and mutant luciferases.

*Key words*: firefly luciferase, luciferin, ATP, bioluminescence spectra, protein structure, computer models, amino acid mutation

Firefly luciferase (luciferin 4-monooxygenase (ATP hydrolysis); luciferin:oxygen 4-oxidoreductase (decarboxylation, ATP hydrolysis), EC 1.13.12.7) catalyzes oxidation of firefly luciferin by oxygen in air in the presence of MgATP [1]. The reaction product, singlet electronically excited oxyluciferin, emits visible light upon transition into the ground state with a quantum yield of ~90% [2]. The amino acid sequences for more than 20 luciferases from several species of fireflies and beetles are now known. The chemistry of the reaction and the emitter structure are identical for all the luciferases isolated. The main difference is the color of the bioluminescence. In nature, the bioluminescence maximum ($\lambda_{max}$) varies from 536 to 638 nm for different species of fireflies [3-5]. In the reaction *in vitro*, the $\lambda_{max}$ coincides with $\lambda_{max}$ *in vivo* at neutral pH, but shifts to the red region with decreasing pH [6]. For some mutant luciferases, red shifts are observed at neutral pH, too. The main factor that determines the $\lambda_{max}$ value is the microenvironment of the emitter, which is located in the enzyme active site. Elucidation of relationships between the luciferase structure and the bioluminescence $\lambda_{max}$ is of both theoretical and practical interest because luciferases and their genes are widely used as markers for the investigation of various biochemical processes *in vitro* and *in vivo* [7, 8] and as highly specific and active bioanalytical reagents [9].

To explain the variations of the bioluminescence $\lambda_{max}$ for native and mutant luciferases, several mechanisms have been proposed in the literature [10]. According to the prevalent mechanism, the changes in bioluminescence spectra, especially at different pH, result from the keto–enol tautomerization of oxyluciferin [11]. As shown in Fig. 1, the C5 proton of the thiazole cycle forms a hydrogen bond with a side residue of the amino acid ($B_1$) that is acting as a base accepting the C5 proton. The oxygen atom of the ketone group interacts with the protonated base ($B_2$) and accepts the proton from the base. Thus, the keto–enol tautomerization is a synchronous transition of the two protons: one proton from the C5 atom of oxyluciferin to $B_1$ base, and second one from $B_2$ base to the oxygen atom of the carbonyl group. The tautomerization results in enol formation. The efficiency of this process depends on the correctness of the fixation of the $B_1$ and $B_2$ bases in the proximity of the oxyluciferin thia-

* To whom correspondence should be addressed.

0006-2979/05/7011-1262 ©2005 Pleiades Publishing, Inc.

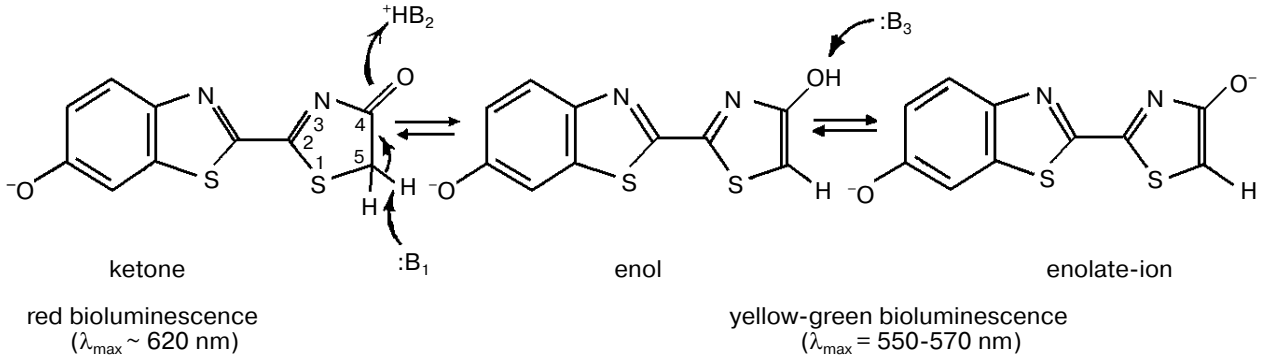


**Fig. 1.** Different forms of electronically exited oxyluciferin: ketone, enol, and enolate-ion.

zole cycle. The interaction of the enolic hydroxyl group with $B_3$ base results in the formation of enolate ion. If $B_1$ base (independently of pH) is absent or protonated (for example, at pH < 6.0), the keto-form of oxyluciferin is observed with bioluminescence maximum in red region of the spectrum. At intermediate pH values, both spectral components, ketone and enol, are observed. The authors of all previously published papers noted only the location of the bioluminescence maximum, but did not analyze changes in the shape of the spectrum. Moreover, it was tacitly assumed that the emission spectra of the enol and the enolate-ion are practically identical [10].

The goal of this work was to study pH dependence of bioluminescence spectra of the wild-type recombinant *Luciola mingrelica* firefly luciferase and its mutant form with the His433Tyr point mutation, quantitative estimation of the contribution of different oxyluciferin forms into these spectra, and elucidation of the role of the protein in the observed differences of bioluminescence spectra for the wild-type and mutant luciferases. Earlier [12], the mutant form of luciferase from Japanese firefly *Hotaria parvula* with bioluminescence maximum in the red region of the spectrum and high catalytic activity was obtained by random mutagenesis. Gene sequencing showed that the mutant enzyme contains the His433Tyr point mutation. Since the amino acid sequences of the luciferases from *H. parvula* and *L. mingrelica* fireflies have homology as high as 98% [13], one could expect that the His433Tyr mutation of *L. mingrelica* luciferase, which is under investigation in our laboratory, will also result in the shift of bioluminescence maximum to the red region of the spectra. In addition, this mutation was chosen because the His433 residue is located at the distance of 12 Å from the enzyme active site, and its mutation cannot have a strong effect on the catalytic properties of the enzyme. According to the literature data [14], even if mutations of amino acid residues in firefly luciferase active center changed the bioluminescence spectra, they at the same time decreased its catalytic activity by dozens and even hundreds of times, which could impede the analysis of spectral characteristics of wild type and mutant enzymes.

## MATERIALS AND METHODS

Restrictases (*Nhe*I, *Kpn*I, *Aat*II), $T_4$ DNA ligase, and Pwo DNA polymerase were from New England Biolabs (USA). *Luciola mingrelica* firefly luciferase was isolated from *E. coli* cells (strain LE 392) carrying the pLR plasmid with the wild-type or mutant (His433Tyr) luciferase gene and purified as described in [15]. All other chemicals were of analytical grade. All solutions were prepared with Milli-Q water (Millipore, France). Site-directed mutagenesis was performed by the PCR method on a Techne (Sweden) PHC-2 amplifier. The pLR plasmid (6270 bp) carrying *L. mingrelica* luciferase gene was isolated from *E. coli* cells, strain LE 392, using Qiagen (USA) kits and used for mutagenesis. Two DNA fragments having overlapping ends were synthesized in the first step and then joined in a fusion reaction. The fusion product was amplified by PCR. The pLR plasmid and the amplified fragment (1820 bp) containing the mutant luciferase gene were treated with restriction enzymes to obtain sticky ends. The non-mutant luciferase gene was cut from the DNA fragment obtained from the pLR plasmid in the previous step. Both DNA fragments were purified and ligated to obtain the m-pLR plasmid vector containing the mutant luciferase gene. Competent *E. coli* cells were transformed with the m-pLR plasmid and grown on Petri dishes with LB medium with ampicillin. Luciferin solution with pH 5.0 was added to the dishes and the colonies were visually checked for bioluminescence. The two brightest colonies were chosen and used for the preparation of mutant luciferase. The m-pLR plasmid was isolated from *E. coli* cells and sequenced to confirm mutation sites corresponding to the His433Tyr replacement.

The bioluminescence spectra were recorded on an LS 50B spectrofluorimeter (Perkin-Elmer, UK). To obtain a bioluminescence spectrum, 2 ml of 0.05 M Tris-

acetate buffer (pH 5.6-10.2) containing 2 mM EDTA, 10 mM $MgSO_4$, 1 mM ATP, and 0.25 mM luciferin were put into a fluorimeter cell, then 0.1 ml of concentrated luciferase solution was added, and the bioluminescence spectrum was recorded in the 500-650 nm interval. The spectrum was corrected for the photomultiplier sensitivity using the instrument software.

Gauss multi-peak fitting of the bioluminescence spectra for the spectra of individual emitters was performed using the Microcal Origin 6.0 Professional program.

Computer models of structures were obtained using the Insight II program (Accelrys Inc., USA). Structure minimization was carried out using AMBER force field [16, 17].

## RESULTS AND DISCUSSION

**The pH dependence of the bioluminescence spectra.** At pH 7.8 (pH optimum for activity of the native enzyme), the bioluminescence $\lambda_{max}$ is at 566 nm for the wild-type luciferase and at 606 nm for the mutant luciferase (Fig. 2). Thus, the His433Tyr point mutation shifted the $\lambda_{max}$ by 40 nm to the red region of the spectrum. We obtained the bioluminescence spectra for the wild-type and mutant luciferases in the pH interval from 5.6 to 10.2. For the wild-type luciferase, yellow-green bioluminescence ($\lambda_{max}$ = 570 nm) was observed at pH ≥ 7.0 and red bioluminescence ($\lambda_{max}$ = 618 nm) at pH = 5.6. Both forms are present at intermediate pH values (Fig. 3a). For the mutant luciferase, red bioluminescence is observed at pH ≤ 6.1. A shoulder in the yellow-green region appears with increase in pH and the bioluminescence intensity in the shoulder increases with increasing pH. Yellow-green bioluminescence prevails over the red bioluminescence only at pH ~ 10.2 (Fig. 3b). The comparison of the pH dependences of bioluminescence spectra shows that the shift in $\lambda_{max}$ of bioluminescence observed at the pH optimum of the catalytic activity (pH 7.8) is explained by the change in the ratio between the different forms of oxyluciferin.

The bioluminescence spectra at different pH values were so far considered as a superposition of spectra for two oxyluciferin forms: ketone and enol, with the $\lambda_{max}$ of bioluminescence at 550-570 and 618 nm, respectively [6,

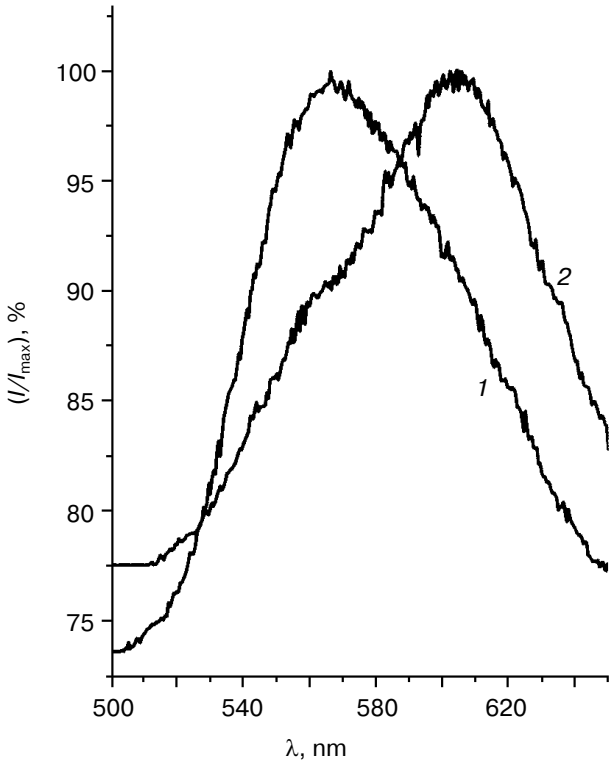


**Fig. 2.** Bioluminescence spectra of wild-type (*1*) and mutant luciferase (*2*) from firefly *L. mingrelica* at pH 7.8. The intensities at the maximum are normalized.

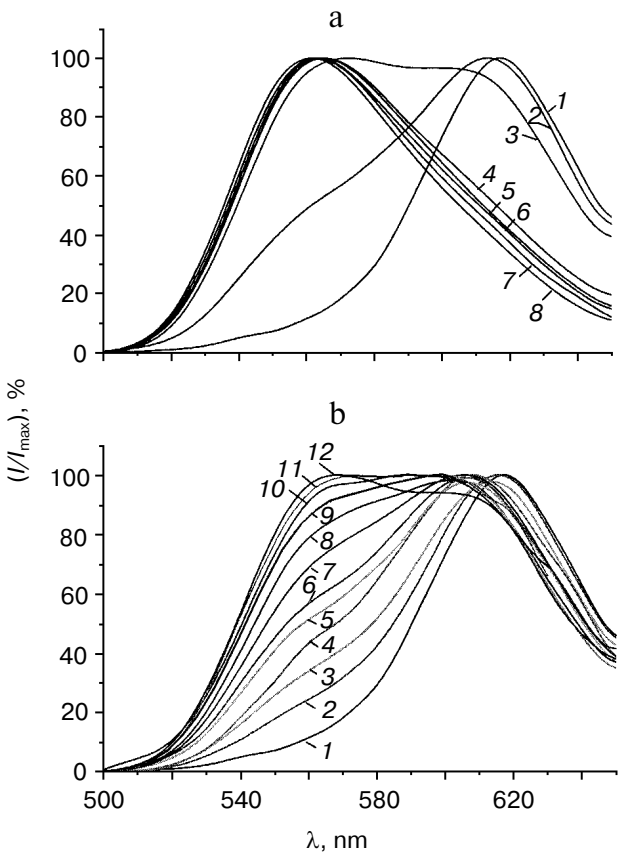


**Fig. 3.** Bioluminescence spectra of wild-type (a) and mutant luciferase (b) from firefly *L. mingrelica* at different pH values: a) 5.6, 6.4, 6.8, 7.0, 7.6, 7.8, 8.0, 8.5 (curves *1-8*, respectively); b) 5.6, 6.1, 6.4, 7.2, 7.6, 7.8, 8.0, 8.6, 8.9, 9.2, 9.6, 10.2 (curves *1-12*, respectively). The intensities in maximum of each spectrum are normalized.

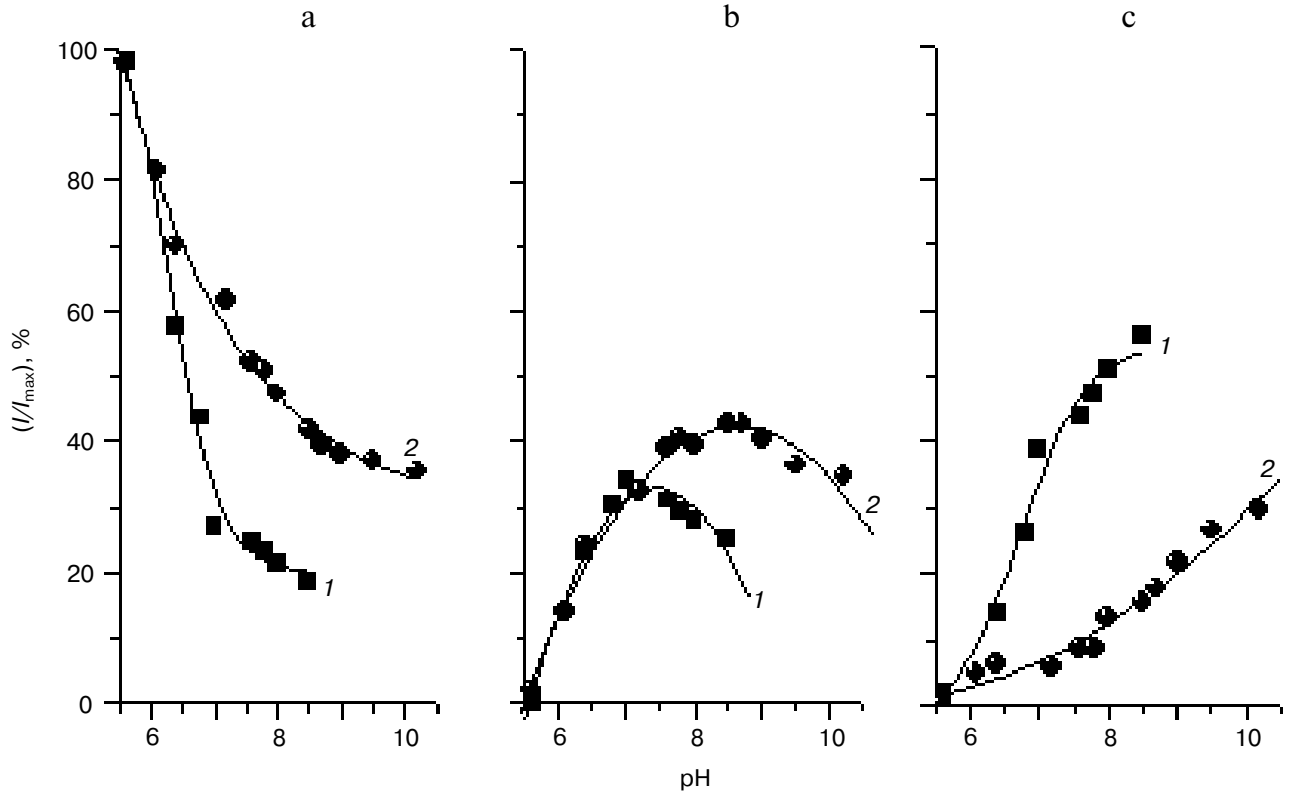


**Fig. 4.** The pH dependence of the relative content (%) of ketone (a), enol (b), and enolate-ion (c) for the wild-type (*1*) and mutant (*2*) firefly luciferases.

10]. However, Gaussian multi-peak fitting using these two forms gives very low correlation coefficient indicating that this model does not correspond to the experimental data. In this connection, we proposed that the spectra of the enolate ion and the enol have different maxima, and the observed bioluminescence spectrum is a superposition of the three forms of electronically exited oxyluciferin rather than two. We found from the experimental data that the enolate ion has $\lambda_{max} = 556$ nm and the ketone has $\lambda_{max} = 618$ nm. Gaussian multi-peak fitting of the bioluminescence spectra revealed the third form of oxyluciferin, i.e., enol, with $\lambda_{max} = 587$ nm. In this case, the correlation coefficient was 0.999, which confirms the validity of our interpretation of the bioluminescence spectra.

Integrating the areas under the bioluminescence spectra for each of the three forms of oxyluciferin under the assumption that the bioluminescence quantum yields of all three emitter forms are nearly the same, we found the relative content of the each form at different pH values (Fig. 4). For the wild-type luciferase, the relative content of ketone decreases to 20% with the increase in pH and remains practically unchanged at pH > 7.0. For the mutant luciferase, the ketone content decreases to 40% as pH increases and does not further change. The relative content of the enol reaches its maximum at pH 7.0 for the wild-type luciferase and at pH 8.6 for the mutant. The relative content of the enolate ion reaches 60% at pH ≥ 7.0 for the wild-type luciferase, whereas this value increases only to 30% even at alkaline pH for the mutant luciferase. Thus, the observed changes in the pH dependence of the bioluminescence spectra of the mutant luciferase in comparison with that of the wild-type luciferase are due to shifts in the ketone ↔ enol ↔ enolate equilibria. Change in the relative content of different emitter forms with change in pH results in the changes of both $\lambda_{max}$ and the shape of the bioluminescence spectrum.

**Mechanism of the changes in bioluminescence spectra upon mutation.** To elucidate the role of amino acid residues of the enzyme active site in the keto–enol tautomerization, we constructed a computer model of the structure of the luciferase–oxyluciferin–AMP complex using the following operations with minimized structure of luciferase–luciferin–ATP complex [18]. Using a molecular editor, the luciferin molecule was transformed into one of the oxyluciferin forms (ketone or enol), and the ATP molecule was transformed into AMP. $Mg^{2+}$ and pyrophosphate were removed from the system. Partial charges in the AMP and oxyluciferin molecules were cal-

culated by the MNDO semi-empirical quantum chemistry method [19] using the AMPAC 6.0 program. Then the coordinates of oxyluciferin, luciferase amino acid residues located at distances less than 6 Å from oxyluciferin, and the AMP molecule were allowed to relax (500 energy minimization steps) into equilibrium with the environment. It is necessary to note that the distance between the oxyluciferin molecule and the His433 residue is about 12 Å in the considered model of luciferase structure. For this reason, the local equilibration of the luciferase active site did not influence the His433 conformation, which was determined by its local environment.

The constructed computer model of the luciferase–oxyluciferin–AMP complex is shown in Fig. 5. The amino acid residues of the *L. mingrelica* firefly luciferase His247, Thr345, Thr529, and Lys531, which are absolutely conserved in all luciferases, are located at distances less than 5 Å from the thiazole ring of oxyluciferin. The oxygen atom of the Thr345 hydroxyl group is near the C-5 proton of oxyluciferin, whereas the imidazole ring of His247 is located near the oxygen atom of the ketone group. These two groups are probably involved in the keto–enol tautomerization process. This supposition agrees well with literature data on mutagenesis of these residues in the luciferase from *P. pyralis* firefly [14]. The mutant with Thr343Ala replacement (according to the numeration for *P. pyralis* luciferase) had bioluminescence maximum in the red region ($\lambda_{max}$ = 617 nm) independent of pH, whereas the His245Arg, Phe, Ala, Gln, and Asn replacements resulted in significant widening of the bioluminescence spectra and change in their pH

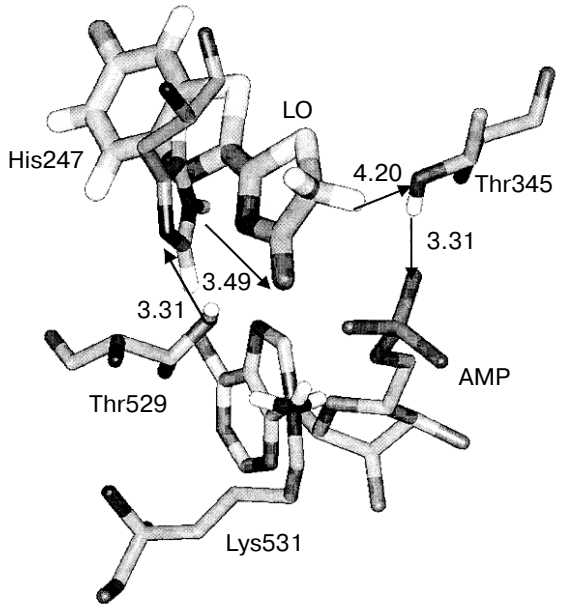


**Fig. 5.** Computer model of the luciferase–oxyluciferin–AMP complex.

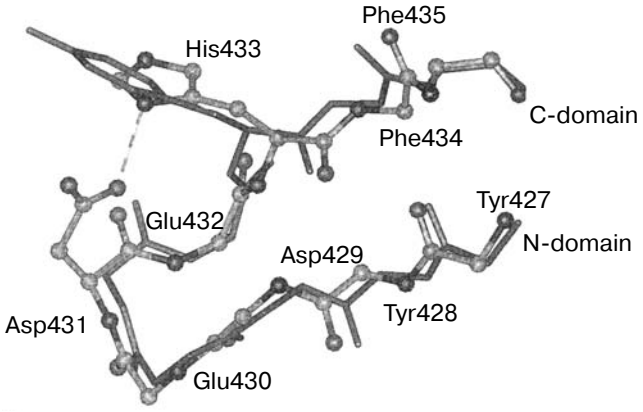


**Fig. 6.** Computer model of the structure of the microenvironment of residue 433 (polypeptide chain Tyr427-Phe435) in the wild-type (ball-and-stick model) and mutant (stick model) firefly luciferases of *L. mingrelica*. The hydrogen bond between His433 and Asp431 residues of the wild-type luciferase is shown by the dashed line.

dependences. His247 and Thr345 residues form hydrogen bonds with Thr529 and Lys531 residues of the luciferase C domain that are also necessary for the tautomerization process. Thus, the change in localization of key amino acid residues and some loosening of the protein structure in the vicinity of the thiazole ring of oxyluciferin results in the equilibrium shift to the enol and ketone.

A question arises: how can the point mutation (His433Tyr) of the residue located at the distance 12 Å from the active site affect the bioluminescence spectra? We are finding the answer on this question upon the examination of the computer model of the environment structure of His433 residue (Fig. 6). Computer modeling of the spatial structure changes upon the His433Tyr replacement was performed starting from the luciferase structure proposed in [18]. The His433Tyr replacement was performed using standard functions provided in Insight II. Then the structures of the wild-type and mutant luciferases were equilibrated using energetic minimization in AMBER force field [16, 17] consisting of 500 steps. Application of such a gentle relaxation procedure allowed us to maintain the basic features of the luciferase structure proposed in [18]. Comparison of the minimized structures of the wild-type and mutant luciferases showed a significant change in the conformation of residue 433. The Tyr phenyl ring in the mutant luciferase appeared to be rotated by almost 60° relative to the location of the His imidazole ring in the wild-type luciferase. This rotation is caused by two factors. The His433 residue is exposed to solvent, protonated, and forms a hydrogen bond between $N_\sigma$ and $O_{\sigma 1}$ atoms of the Asp431 residue [18]. This hydrogen bond fixes the position of the His ring. Upon the His-Tyr replacement, the

hydrogen bond disappears, and the Tyr phenyl ring turns by 60° in conformity with the local force balance. This turning is observed during the first dozens of minimization steps. The Tyr433 conformation does not change during all the subsequent process of structure equilibration.

The analysis of X-ray data for luciferases, which belong to the group of adenylating enzymes, and other adenylating enzymes showed that the His433 residue is located in a flexible loop formed by the Tyr427-Phe435 residues binding the N and C domains of the luciferase [20, 21]. This loop can be considered as a hinge binding the two luciferase domains. The imidazole cycle of the His433 residue forms a hydrogen bond with the carboxyl group of Asp431 residue, which increases the rigidity of the "hinge" and decreases the thermal fluctuation amplitudes of the N and C domains with respect to each other. This ensures sufficiently rigid fixation of Thr529 and Lys531 amino acid residues of the C domain, which are involved in the nearest environment of the oxyluciferin thiazole group. This hydrogen bond disappears upon the His433Tyr replacement, which decreases the rigidity of the "hinge" Tyr427-Phe435 and increases the amplitude of thermal fluctuations of the domains with respect to each other. This results in a shift of the equilibrium (Fig. 1) to the ketone and enol. Profound effect of the C domain on the form and $\lambda_{max}$ of the bioluminescence spectra is confirmed by the literature data: the mutant luciferase in the absence of the C domain generates only red and very week bioluminescence [22].

In conclusion, it should be stressed that the approach proposed for the analysis of bioluminescence spectra is based on photo-physical concepts about the correlation between bioluminescence spectra on one side and structure of the emitter and its microenvironment on the other. This approach can be rather fruitful for the analysis of bioluminescence spectra of different native and mutant firefly luciferases. Detailed studies of the bioluminescence spectra over a large pH interval, quantitative estimation of the contribution of different forms of the emitter into bioluminescence spectra, and using of data related to the structure of the luciferases and their complexes with substrates and reaction products, as well as computer models, permit one to elucidate the relationship between the bioluminescence spectra features and luciferase structures.

This work was supported by the Russian Foundation for Basic Research (grant No. 02-04-48-961), INTAS (grant No. 2000-562), and CRDF-IPP (RBO-11009(1)-MO-99 (PNNL)).

We thank Professor Kathryn Thomasson (University of North Dakota, USA) for the use of Insight II software.

## REFERENCES

1. McElroy, W. D., and De Luca, M. (1974) in *Chemiluminescence and Bioluminescence* (Cormier, M. J., Hercules, D. M., and Lee, J., eds.) Plenum Press, New York, pp. 285-311.
2. Seliger, H. H., and McElroy, W. D. (1964) *Proc. Natl. Acad. Sci. USA*, **52**, 75-81.
3. Wood, K. V., Lam, Y. A., Seliger, H. H., and McElroy, W. D. (1989) *Science*, **244**, 700-702.
4. Ugarova, N. N. (1989) *J. Biolum. Chemilum.*, **4**, 406-418.
5. Viviani, V. R., Silva, A. C. R., Perez, G. L. O., Santelli, R. V., Bechara, E. J., and Reinach, F. C. (1999) *Photochem. Photobiol.*, **70**, 254-260.
6. Gandelman, O. A., Brovko, L. Yu., Ugarova, N. N., Chikishev, A. Yu., and Shkurinov, A. P. (1993) *J. Photochem. Photobiol., B: Biol.*, **19**, 187-191.
7. Kricka, L. J. (2000) in *Methods in Enzymology. Bioluminescence and Chemiluminescence*, Vol. 305 (Ziegler, M. M., and Baldwin, T. O., eds.) Academic Press, San Diego, pp. 333-345.
8. Ohkuma, H., Abe, K., Kosaka, Y., and Maeda, M. (2000) *Luminescence*, **15**, 21-27.
9. Ugarova, N. N. (1993) *Appl. Biochem. Microbiol. (Moscow)*, **29**, 135-144.
10. Ugarova, N. N., and Brovko, L. Yu. (2002) *Luminescence*, **17**, 321-330.
11. White, E. H., Rapaport, E., Hopkins, T. A., and Seliger, H. H. (1969) *J. Am. Chem. Soc.*, **91**, 2178-2180.
12. Ueda, H., Yamanouchi, H., Kitayama, A., Inoue, K., Hirano, T., Suzuki, E., Nagamune, T., and Ohmiya, Y. (1997) in *Bioluminescence and Chemiluminescence. Molecular Reporting with Photons* (Hastings, J. W., Kricka, L. J., and Stanley, P. E., eds.) John Wiley, Chichester, pp. 216-219.
13. Ohmiya, Y., Ohba, N., Toh, H., and Tsui, F. I. (1995) *Photochem. Photobiol.*, **62**, 309-313.
14. Branchini, B. R., Magyar, R. A., Murtiashaw, M. H., Anderson, S. M., Helgerson, L. C., and Zimmer, M. (1999) *Biochemistry*, **38**, 13223-13230.
15. Lundovskich, I. A., Leontieva, O. V., Dementieva, E. I., and Ugarova, N. N. (1999) in *Bioluminescence and Chemiluminescence. Perspectives for 21st Century* (Roda, A., Pazzagli, M., Kricka, L. J., and Stanley, P. E., eds.) John Wiley, Chichester, pp. 420-424.
16. Weiner, S. J., Kollman, P. A., Case, D. A., Singh, U. C., Ghio, C., Alagona, G., Profeta, S. Jr., and Weiner, P. (1984) *J. Am. Chem. Soc.*, **106**, 765-784.
17. Weiner, S. J., Kollman, P. A., Nguyen, D. T., and Case, D. A. (1986) *J. Comp. Chem.*, **7**, 230-252.
18. Sandalova, T. P., and Ugarova, N. N. (1999) *Biochemistry (Moscow)*, **64**, 962-967.
19. Minkin, V. I., Simkin, B. F., and Minyaev, R. M. (1997) *Theory of Molecular Structure* [in Russian], Feniks, Rostov-on-Don.
20. Conti, E., Franks, N. P., and Brick, P. (1996) *Structure*, **4**, 287-298.
21. Conti, E., Stachelhaus, T., Marahiel, M. A., and Brick, P. (1997) *EMBO J.*, **16**, 4174-4183.
22. Zako, T., Ayabe, K., Aburatani, T., Kamiya, N., Kitayama, A., Ueda, H., and Nagamune, T. (2003) *Biochim. Biophys. Acta, Proteins & Proteomic*, **1649**, 183-189.